Inorganic Chemistry
Article

Inorg. Chem. **2009**, *48*, 8845–8855 **8845**
DOI: 10.1021/ic901026x

Mononuclear and Polynuclear Copper(II) Complexes Derived from Pyridylalkylaminomethylphenol Polypodal Ligands

Jorge Manzur* and Hector Mora

Departamento de Ciencia de los Materiales, Facultad de Ciencias Físicas y Matemáticas, Universidad de Chile, Tupper 2069, Santiago, Chile

Andrés Vega

Departamento de Ciencias Químicas, Facultad de Ecología y Recursos Naturales, Universidad Andres Bello, República 275, Santiago, Chile

Diego Venegas-Yazigi

Departamento de Química de los Materiales, Facultad de Química y Biología, Universidad de Santiago de Chile, Avenida L. B. O'Higgins 3363, Casilla 40-Correo 33, Santiago, Chile

Miguel A. Novak

Instituto de Física, Universidade Federal do Rio de Janeiro, BR-21945970, RJ, Brazil

José Ricardo Sabino

Instituto de Física, Universidade Federal do Goiás, BR-74001970, GO, Brazil

Verónica Paredes-García

Departamento de Química, Universidad Tecnológica Metropolitana, Avenida José Pedro Alessandri 1242, Santiago, Chile

Evgenia Spodine

Departamento de Química Inorgánica y Analítica, Facultad de Ciencias Químicas y Farmacéuticas, Universidad de Chile, Sergio Livingstone 1007, Santiago, Chile

Received May 27, 2009

Four mononuclear complexes $[Cu(HL^1)Cl]PF_6 \cdot CH_3OH$ (**1**), $[Cu(HSL^1)Cl]PF_6 \cdot 0.75H_2O$ (**2**), $[Cu(HL^2)Cl]PF_6 \cdot CH_3OH$ (**3**), $[Cu(HSL^2)Cl]PF_6 \cdot 1.5CH_3OH$ (**4**), and two polynuclear complexes $[Cu_2(SL^2)_2](PF_6)_2 \cdot 2CH_3OH$ (**5**) and $\{Cu[Cu(SL^2)(Cl)]_2\}(PF_6)_2$ (**6**) (HL^1: 2-[(bis(2-pyridylmethyl)-amino)methyl]-4-methylphenol; HSL^1: 2-[(bis(2-pyridylmethyl)amino) methyl]-4-methyl-6-(methyl-thio)phenol; HL^2: 2-[(2-pyridylmethyl)(2′-pyridylethyl)-aminomethyl)]-4-methylphenol; HSL^2: 2-[(2-pyridylmethyl)(2′-pyridylethyl)amino-methyl]-4-methyl-6-(methylthio)phenol were obtained and characterized. The crystal structures of the mononuclear complexes **1**−**4** show the copper centers in a square-base pyramidal environment with the phenolic oxygen coordinated at the axial position. Dinuclear complex **5** has two copper centers with different geometry and bridged by phenoxo oxygens; one of the copper atoms is square pyramidal while the other can be described with a highly distorted octahedral geometry with a long Cu−S distance (2.867 Å). Density functional theory calculations were used to obtain the reported structure of **6**, since single crystals suitable for X-ray diffraction were not isolated. Magnetic studies done for **5** and **6** show an antiferromagnetic behavior for **5** ($J = -134$ cm^{-1}) and a ferromagnetic behavior for **6** ($J = +11.9$ cm^{-1}). Redox potentials for the mononuclear complexes were measured by cyclic voltammetry; the values show the effect of the chelating ring size (−213 mV and −142 mV for Cu-HL^1 and Cu-HL^2, respectively) and the presence of the thiomethyl substituent (−213 mV and −184 mV for Cu-HL^1 and Cu-HSL^1, respectively).

Introduction

Copper coordination complexes have been studied as small molecule analogues of metalloproteins that mediate dioxygen activation, electron transfer, and transport processes. The great importance of the biological activity of copper because of the presence of this ion in enzymes and proteins has increased the interest in the coordination chemistry of copper with O,N-coordinating ligands as mimetic systems. For

*To whom correspondence should be addressed. E-mail: jmanzur@dqb.uchile.cl.

Published on Web 08/17/2009

example, tripodal polydentate amines have been used to prepare copper(I) and copper(II) complexes which serve as model systems of metalloproteins.[1−5] Variations in structural parameters, such as the length of each arm of the tripodal ligand and/or the nature of the donor groups, have been found to have dramatic effects upon the structure, redox potential, and spectroscopic features of the corresponding complexes.[6−9]

To study these parameters several copper(II) complexes with polydentate amines including a phenolic group have been prepared and characterized[10−13] as a model of galactose oxidase. The stability, reactivity, and magnetic properties of these compounds depend on some strongly correlated factors, such as protonation of the phenolic moieties, geometry (axial versus equatorial binding to copper), and electronic properties.[13]

The first example of a complex containing an axially coordinated phenolate moiety from a tripodal ligand, in contrast to the rather common equatorially coordination mode,[14] was reported by Rajendran et al.[15] and Uma[16] et al. for [Cu(bpnp) Cl] [Hbpnp: 2-(bis(pyrid-2-ylmethyl)-aminomethyl)-4-nitrophenol] and by Vaidyanathan et al.[12] for [Cu(bpnp)X] ($X = SCN^-, CH_3COO^-, ClO_4^-$). Another interesting example of a complex with a phenol rather than a deprotonated phenolate in the apical position of a mononuclear complex was reported by Ito et al.[17] for $[Cu(phpyH)]ClO_4$ (phpyH: 2-[(bis(2-pyridylethyl)-amino)-methyl]-4-methylphenol).

In this study we have succeeded in preparing mononuclear copper(II) complexes from polypodal ligands derived from pyridylalkylaminomethylphenol, which are characterized by the diversity of the coordination modes of these ligands, permitting to obtain from mononuclear to polynuclear (di and trinuclear) species. The mononuclear copper(II) complexes present an axial copper(II)-protonated phenolic bond, incorporating different N_3O coordinating tripodal ligands (Scheme 1). The solid structures of the complexes, as well as their properties, were studied by X-ray diffractometry and spectroscopic and electrochemical methods. Besides, a double symmetric phenoxo-bridged dinuclear Cu^{II} complex and a trinuclear one were isolated, and characterized by single crystal X-ray diffraction and by variable-temperature magnetic susceptibility.

Scheme 1. Ligands Used in This Work

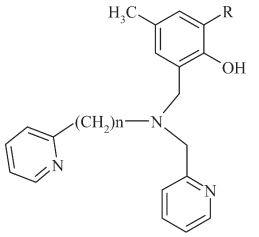

HL^1: R = H n = 1

HSL^1: $R = SCH_3$ n = 1

HL^2: R = H n = 2

HSL^2: $R = SCH_3$ n = 2

Experimental Section

All reagents were reagent grade and used without further purification, unless stated otherwise. Solvents were of HPLC quality and were freshly distilled under nitrogen before use. Acetonitrile (CH_3CN) was distilled from calcium hydride.

Elemental analyses for C, H, and N were performed at CEPEDEQ (University of Chile) on a Fison-Carlo Erba EA 1108 model analyzer. Copper was determined by atomic absorption spectroscopy. IR spectra were obtained neat or as KBr pellets on a Bruker Vector 22 instrument. ^1H NMR spectra were recorded in $CDCl_3$ on a Bruker AMX-300 NMR spectrometer. Chemical shifts are reported as δ values downfield of an internal Me_4Si reference. Cyclic voltammograms were recorded on a BAS CV50−W voltammetric analyzer, using a typical three electrode system, with a glassy carbon as the working electrode, a saturated calomel electrode as reference and a platinum electrode as auxiliary electrode, and 0.1 M tetrabutylammonium hexafluorophosphate as supporting electrolyte. UV−visible spectra were recorded on a Perkin-Elmer Lamda 11 equipment.

Syntheses. Synthesis of Ligands. 2-(Methylthio)-*p*-cresol was prepared from *p*-cresol according to the literature.[18] 2-[(Bis(2-pyridylmethyl)amino)methyl]-4-methylphenol (HL^1), 2-[(bis(2-pyridylmethyl)amino) methyl]-4-methyl-6-(methylthio)-phenol (HSL^1), 2-[(2-pyridylmethyl)(2′-pyridylethyl)-aminomethyl)]-4-methylphenol, HL^2 and 2-[(2-pyridylmethyl)(2′-pyridylethyl)amino-methyl]-4-methyl-6-(methylthio)phenol, HSL^2 were synthesized by a Mannich reaction with bis(2-pyridylmethyl)amine,[19] (2-pyridylmethyl)(2-pyridylethyl)amine,[19] paraformaldehyde, and *p*-cresol or 2-(methylthio)-*p*-cresol, in 50, 57, 62, and 63% yields, respectively, as described for similar ligands.[20]

General Method. To a paraformaldehyde suspension (35 mmol) in methanol (27 mL) the (2-pyridyl)amine was added

(1) *Copper Coordination Chemistry: Biochemical and Inorganic Perspectives*; Karlin, K. D., Zubieta, J., Eds.; Adenine Press: New York, 1983.
(2) Rorabacher, D. B. *Chem. Rev.* **2004**, *104*, 651–697.
(3) Mirica, L. M.; Ottenwaelder, X.; Stack, D. P. *Chem. Rev.* **2004**, *104*, 1013–1045.
(4) Lewis, E. A.; Tolman, W. B. *Chem. Rev.* **2004**, *104*, 1047–1076.
(5) Lee, D.-H.; Hatcher, L. Q.; Vance, M. A.; Sarangi, R.; Milligan, A. E.; Sarjeant, A. A. N.; Incarvito, C. D.; Rheingold, A. L.; Hodgson, K. O.; Hedman, B.; Solomon, E. I.; Karlin, K. D. *Inorg. Chem.* **2007**, *46*, 6056–6068.
(6) Karlin, K. D.; Sherman, S. E. *Inorg. Chim. Acta* **1982**, *65*, L39–L40.
(7) Karlin, K. D.; Hayes, J. C.; Juen, S.; Hutchinson, J. P.; Zubieta, J. *Inorg. Chem.* **1982**, *21*, 4106–4108.
(8) Ambundo, E. A.; Deydier, M.-V.; Grall, A. J.; Aguera-Vega, N.; Dressel, L. T.; Cooper, T. H.; Heeg, M. J.; Ochrymowycz, L. A.; Rorabacher, D. B. *Inorg. Chem.* **1999**, *38*, 4233–4242.
(9) Ambundo, E. A.; Deydier, M.-V.; Ochrymowycz, L. A.; Rorabacher, D. B. *Inorg. Chem.* **2000**, *39*, 1171–1179.
(10) Shimazaki, Y.; Huth, S.; Hirota, S.; Yamauchi, O. *Bull. Chem. Soc. Jpn.* **2000**, *73*, 1187–1195.
(11) Shimazaki, Y.; Huth, S.; Hirota, S.; Yamauchi, O. *Inorg. Chim. Acta* **2002**, *331*, 168–170.
(12) Vaidyanathan, M.; Viswanathan, R.; Palaniandavar, M.; Balasubramanian, T.; Prabhaharan, P.; Muthiah, T. P. *Inorg. Chem.* **1998**, *37*, 6418–6427.
(13) Philibert, A.; Thomas, F.; Philouze, C.; Hamman, S.; Saint-Aman, E.; Pierre, J.-L. *Chem.—Eur. J.* **2003**, *9*, 3803–3812.
(14) (a) Adams, H.; Bailey, N. A.; Fenton, D. E.; He, Q.-Y.; Ohba, M.; Okawa, H. *Inorg. Chim. Acta* **1994**, *215*, 1. (b) Adams, H.; Bailey, N. A.; Rodriguez de Barbarin, C. O.; Fenton, D. E.; He, Q.-Y. *J. Chem. Soc., Dalton Trans.* **1995**, 2323.
(15) Rajendran, U.; Viswanathan, R.; Palaniandavar, M.; Lakshminarayanan, M. *J. Chem. Soc., Dalton Trans.* **1992**, 3563.
(16) Uma, R.; Viswanathan, R.; Palaniandavar, M.; Lakshminarayanan, M. *J. Chem. Soc., Dalton. Trans.* **1994**, 1219.
(17) Ito, S.; Nishino, S.; Itoh, H.; Ohba, S.; Nishida, Y. *Polyhedron* **1998**, *17*, 1637–1642.
(18) Farrah, B. S.; Gilbert, E. E. *J. Org. Chem.* **1963**, *28*, 2807–2809.
(19) Rojas, D.; García, A. M.; Vega, A.; Moreno, Y.; Venegas-Yazigi, D.; Garland, M. T.; Manzur, J. *Inorg. Chem.* **2004**, *43*, 6324–6330.
(20) Itoh, S.; Takayama, S.; Arakawa, R.; Furuta, A.; Komatsu, M.; Ishida, A.; Takamuku, S.; Fukuzumi, S. *Inorg. Chem.* **1997**, *36*, 1407–1416.

(25.12 mmol), and the mixture was refluxed for 1 h. A solution of the corresponding substituted phenol (25.12 mmol) in methanol (8 mL) was added, and the mixture was refluxed for additional 14 h, under nitrogen. After removing the solvent under vacuum, the brown residue was purified by column chromatography (silica-gel) using chloroform as eluent, followed by a 5% methanol/chloroform mixture.

^{1}H NMR Data. HL^1: 10.8 (1H, broad, OH), 8.54 (2H, d, pyridine Hα), 7.58 (2H, t), 7.31 (2H, d) and 7.12 (2H, t) (pyridine protons), 6.95 (1H, d), 6.85 (1H, s), 6.80 (1H, d) (phenyl protons), 3.85 (4H, s, CH_2-Py), 3.73 (2H, s, CH_2-Ph), 2.21 (3H, s, CH_3-Ph).

HSL^1: 11.4 (1H, broad, OH), 8.58 (2H, d, pyridine Hα), 7.63 (2H, t), 7.36 (2H, d) and 7.16 (2H, t, pyridine protons), 6.92 (1H, s), and 6.72 (1H, s, phenyl protons), 3.86 (4H, s, CH_2-Py), 3.75 (2H, s, CH_2-Ph), 2.46 (3H, s, CH_3-S), 2.26 (3H, s, CH_3-Ph).

HL^2: 10.2 (1H, broad, OH), 8.57 and 8.49 (2H, d, pyridine Hα), 7.60 and 7.56 (2H, t), 7.19 (2H, d) and 7.11 (2H, m, pyridine protons), 7.07 (1H, d), 6.96 (1H, d), 6.83 (1H, s), 6.74 (1H, d, phenyl protons), 3.87 (2H, s, CH_2-Py), 3.84 (2H, s, CH_2-Ph), 3.05 (4H, m, CH_2-CH_2), 2.24 (3H, s, CH_3-Ph).

HSL^2: 8.54 and 8.46 (2H, d, pyridine Hα), 7.60 and 7.54 (2H, t), 7.23 and 7.05 (2H, d), 7.15 and 7.09 (2H, t, pyridine protons), 6.88 and 6.65 (2H, s, phenyl protons), 3.87 (2H, s, CH_2-Py), 3.80 (2H, s, CH_2-Ph), 3.0 (4H, m, CH_2-CH_2), 2.41 (3H, s, CH_3-S), 2.23 (3H, s, CH_3-Ph).

Synthesis of Complexes. Mononuclear Complexes. The mononuclear copper(II) complexes were obtained by reaction of a solution of the appropriate ligand in methanol with copper dichloride in equimolar ratio. The resulting mixture was refluxed for 1 h, and then an excess of tetrabutylammonium hexafluorophosphate was added. The solid that separates was filtered, washed with cold methanol, and dried under vacuum. Suitable crystals for X-ray diffraction studies were obtained from hot methanol. The complexes were characterized by X-ray diffraction, elemental analysis, and cyclic voltammetry.

$[Cu(HL^1)Cl]PF_6\cdot CH_3OH$ (1). Yield 88%. Elemental analysis: Calcd for $C_{21}H_{25}ClCuF_6N_3O_2P$: C: 42.33; H: 4.23; N: 7.06; Cu: 10.67%. Found: C: 41.5; H: 4.4; N: 7.2; Cu: 11.0%.

$[Cu(HSL^1)Cl]PF_6\cdot 0.75H_2O$ (2). Yield 93%. Elemental analysis: Calcd for $C_{21}H_{24.5}ClCuF_6N_3O_{1.75}PS$: C: 40.46; H: 3.97; N: 6.74; Cu: 10.20%. Found: C: 41.0; H: 3.9; N: 6.9; Cu: 10.5%.

$[Cu(HL^2)Cl]PF_6\cdot CH_3OH$ (3). Yield 92%. Elemental analysis: Calcd for $C_{22}H_{27}ClCuF_6N_3O_2P$: C: 43.33; H: 4.47; N: 6.89; Cu: 10.42%. Found: C: 44.0; H: 4.7; N: 7.1; Cu: 11.2%.

$[Cu(HSL^2)Cl]PF_6\cdot 1.5CH_3OH$ (4). Yield 64%. Elemental analysis: Calcd for $C_{23.5}H_{31}ClCuF_6N_3O_{2.5}PS$: C: 42.0; H: 4.65; N: 6.26; Cu: 9.46%. Found: C: 43.1; H: 4.6; N: 6.2; Cu: 9.8%.

Polynuclear Complexes. The dinuclear copper(II) complex $[Cu(SL^2)_2](PF_6)_2\cdot 2\,CH_3OH$ (**5**) and trinuclear copper(II) complex $\{Cu[Cu(SL^2)(Cl)]_2\}(PF_6)_2$ (**6**) were obtained by reaction of a solution of the appropriate ligand in methanol with copper dichloride in a 2:1 and 3:2 metal to ligand ratio, respectively, in the presence of triethylamine as base. The mixture was refluxed for 1 h, and then an excess of tetrabutylammonium hexafluorophosphate was added. The solid that separates was filtered, washed with cold methanol, and dried under vacuum.

$[Cu_2(SL^2)_2](PF_6)_2\cdot 2CH_3OH$ (5). Yield 72%. Suitable crystals for X-ray diffraction studies were obtained from hot methanol. The complex was characterized by X-ray diffraction, elemental analysis, and cyclic voltammetry.

Elemental analysis: Calcd for $C_{46}H_{56}Cu_2F_{12}N_6O_4P_2S_2$: C: 44.59; H: 4.56; N: 6.79; Cu: 10.26%. Found: C: 44.0; H: 4.4; N: 7.2; Cu: 10.2%.

$\{Cu[Cu(SL^2)(Cl)]_2\}(PF_6)_2$ (6). Yield 97%. Despite efforts to produce single crystals suitable for X-ray diffraction, these were not obtained, and a computational optimization of the structure was done. The compound was characterized by elemental analysis, and cyclic voltammetry.

Elemental analysis: Calcd for $C_{44}H_{48}Cl_2Cu_3F_{12}N_6O_2P_2S_2$: C: 40.36; H: 3.70; N: 6.42; Cu: 14.56%. Found: C: 40.0; H: 3.6; N: 6.6; Cu: 14.2%.

X-ray Crystallographic Data Collection and Refinement of the Structures. For each compound a single crystal was mounted on a glass fiber, except for compound $[Cu(HSL^2)Cl]PF_6$ (**4**) which loses solvent at room temperature; consequently it was measured inside a sealed capillary tube containing mother liquor. The intensity data collection was made on a Bruker Smart Apex diffractometer, using separations of 0.3° between frames and 10 s by frame. Compounds **1**−**3** and **5** were measured at room temperature, while the diffraction intensities for **4** were collected at 100 K. Data integration was made using SAINTPLUS.[21] The structures were solved by direct methods using XS in SHELXTL[22] and completed (non-H atoms) by Fourier difference synthesis. Refinement until convergence was obtained using XL SHELXTL[23] and SHELXL97.[23] All hydrogen atoms (with the exception of those of the phenol group) were calculated in idealized positions on geometric basis and refined with restrictions. The hydrogen atoms of the phenol groups (OH) for compounds **1**−**4** were located in the Fourier difference map in the final stages of refinement. Subsequently they were not refined. Additional crystallographic and refinement details are given in Table 1.

During the final stages of the refinement of compounds **1**, **2**, and **4** some disorder in the hexafluorophosphate counteranion was noticed. It was modeled considering two positions, A and B, with partial occupations adding up to 1. These were refined and held constant in the final cycles of refinement. The occupation values for A and B were 0.63/0.37, 0.52/0.48, and 0.60/0.40 for **1**, **2**, and **4**, respectively. The P−F distance for these three compounds was restricted to be a parameter, varied during refinement and held constant during the last refinement cycles.

During the structure completion process by difference Fourier synthesis of compound **4** and **5**, it was clear that some ill defined electron density was present in the holes of the structure left by the molecules and PF_6^- counteranions. Efforts to modelate this density as solvent molecules or disordered solvent molecules failed. Finally, the remaining and unassigned electron density was modeled using Platon SQUEEZE,[24] a method allowing a good modeling of unresolved electron density.[25] It leads to $46e^-$ for the unitary cell of **4** and 120 for **5**. Considering this, three and eight methanol molecules by unit cell were computed for the reported formula of **4** and **5**, respectively.

DFT Calculations. Density functional theory (DFT) calculations were carried out using the Amsterdam Density Functional package[26a] developed by Baerends and co-workers.[26b−f] The local density approximation for electron correlation was treated with the Vosko−Wilk−Nusair parametrization.[27] The nonlocal corrections of Becke[28,29] and Perdew[30,31] (BP86) were added to the exchange and correlation energies, respectively. The numerical integration procedure applied for the calculations was developed by te Velde et al.[26f] The standard ADF STO TZP basis set was used.[26a] The

(21) *SAINTPLUS*, Version 6.02; Brucker AXS: Madison, WI, 1999.
(22) *SHELXTL*, Version 5.1; Brucker AXS: Madison, WI, 1998.
(23) Sheldrick, G. M. *SHELXL-97, Program for Crystal Structure Refinement*; University of Göttingen: Göttingen, Germany, 1997.
(24) Spek, A. L. *J. Appl. Crystallogr.* **2003**, *36*, 7–13.
(25) Cheruzel, L. E.; Cecil, M. R.; Edison, S. E.; Mashuta, M. S.; Baldwin, M. J.; Buchanan, R. M. *Inorg. Chem.* **2006**, *45*, 3191–3202.
(26) (a) *ADF2002.01*; Theoretical Chemistry, Vrije Universiteit: Amsterdam, The Netherlands, SCM (http://www.scm.com); (b) Baerends, E. J.; Ellis, D. E.; Ros, P. *Chem. Phys.* **1973**, *2*, 41–51. (c) Velde, G. te; Baerends, E. J. *J. Comput. Phys.* **1992**, *99*, 84–98. (d) Fonseca Guerra, C.; Snijders, J. G.; Velde, G. te; Baerends, E. *J. Theor. Chim. Acc.* **1998**, *99*, 391–403. (e) Bickelhaupt, F. M.; Baerends, E. J. *Rev. Comput. Chem.* **2000**, *15*, 1–86. (f) te Velde, G.; Bickelhaupt, F. M.; Fonseca Guerra, C.; van Gisbergen, S. J. A.; Baerends, E. J.; Snijders, J. G.; Ziegler, T. *J. Comput. Chem.* **2001**, *22*, 931–967.
(27) Vosko, S. D.; Wilk, L.; Nusair, M. *Can. J. Phys.* **1980**, *58*, 1200–1211.
(28) Becke, A. D. *J. Chem. Phys.* **1986**, *84*, 4524–4529.
(29) Becke, A. D. *Phys. Rev. A.* **1988**, *38*, 3098–3100.
(30) Perdew, J. P. *Phys. Rev. B* **1986**, *33*, 8822–8824.
(31) Perdew, J. P. *Phys. Rev. B* **1986**, *34*, 7406E.

Table 1. Structure and Refinement Details for $[Cu(HL^1)Cl]PF_6 \cdot CH_3OH$ (**1**), $[Cu(HSL^1)Cl]PF_6 \cdot 0.75H_2O$ (**2**), $[Cu(HL^2)Cl]PF_6 \cdot CH_3OH$ (**3**), $[Cu(HSL^2)Cl]PF_6 \cdot 1.5CH_3OH$ (**4**), and $[Cu_2(SL^2)_2](PF_6)_2 \cdot 2CH_3OH$ (**5**)

	1	**2**	**3**	**4**	**5**
formula	$C_{21}H_{25}ClCuF_6N_3O_2P$	$C_{21}H_{24.5}ClCuF_6N_3O_{1.75}PS$	$C_{22}H_{27}ClCuF_6N_3O_2P$	$C_{23.5}H_{31}ClCuF_6N_3O_{2.5}PS$	$C_{46}H_{56}Cu_2F_{12}N_6O_4P_2S_2$
weight	595.41	622.98	609.43	671.42	1237.89
color, habit	blue, plate	blue, polyhedron	blue, block	blue, block	blue, plate
size/mm^3	$0.37 \times 0.13 \times 0.04$	$0.41 \times 0.22 \times 0.10$	$0.63 \times 0.50 \times 0.48$	$0.20 \times 0.15 \times 0.12$	$0.10 \times 0.10 \times 0.04$
crystal system	monoclinic	triclinic	triclinic	triclinic	monoclinic
space group	$P2_1/n$	$P\bar{1}$	$P\bar{1}$	$P\bar{1}$	$P2_1/c$
a/Å	11.7035(12)	9.813(5)	9.2321(15)	10.315(2)	12.8364(11)
b/Å	9.5410(9)	11.233(5)	12.555(2)	12.571(3)	19.5117(16)
c/Å	22.441(2)	13.437(6)	13.499(2)	13.225(3)	21.4151(18)
α/deg	90	103.763(8)	103.169(2)	62.76(3)	90
β/deg	97.221(2)	108.408(8)	109.726(2)	67.19(3)	105.061(2)
γ/deg	90	99.987(8)	109.018(2)	89.55(3)	90
volume/Å^3	2486.0(4)	1314.5(11)	1288.2(4)	1375.0(5)	5179.4(8)
Z	4	2	2	2	4
D_c/kgm^{-3}	1.591	1.584	1.571	1.603	1.526
μ/mm^{-1}	1.120	1.140	1.082	1.093	1.051
T_{min}, T_{max}	0.68, 0.96	0.65, 0.90	0.59, 0.63	0.82, 0.88	0.90, 0.96
$F(000)$	1212	637	622	676	2428
2θ range	1.83 to 25.01	1.68 to 25.29	1.73 to 25.07	1.86 to 23.77	1.64 to 26.61
index ranges	$-13 \le h \le 13$	$-11 \le h \le 11$	$-10 \le h \le 10$	$-11 \le h \le 11$	$-16 \le h \le 14$
	$-11 \le k \le 11$	$-13 \le k \le 13$	$-16 \le k \le 14$	$-13 \le k \le 13$	$-24 \le k \le 24$
	$-25 \le l \le 26$	$-15 \le l \le 15$	$-16 \le l \le 15$	$-14 \le l \le 14$	$-25 \le l \le 25$
least squares refl.	4365	4661	4522	3980	10679
parameters	383	390	332	393	637
R[a]	0.0569	0.0787	0.0409	0.0511	0.0576
wR[b]	0.1257	0.1854	0.1049	0.1518	0.1620
S	1.042	1.050	1.047	1.072	1.066
max., min diff./ e Å^{-3}	0.636, −0.293	0.736, −0.397	0.436, −0.260	0.786 to −0.754	2.491 to 1.375

[a] $R = \sum||F_o| - |F_c||/\sum|F_o|$. [b] $R_w = [\sum w(|F_o| - |F_c|)^2/\sum w(F_o)^2]^{1/2}$, where $w = 1/\sigma^2(F_o)$, λ(Mo Kα) = 0.71073.

frozen-core approximation[32] was considered for Cu, 3p; S, 2p; Cl, 2p; F, O, N, and C, 1s.

The geometry of compound $\{Cu[Cu(SL^1)(Cl)]_2\}(PF_6)_2$,[33] obtained from the X-ray diffraction data, was considered as a model for constructing the starting point for optimization. Two different guess structures were used, leading in both cases to the same final optimized geometry. Thus, the geometry of $\{Cu[Cu(SL^1)(Cl)]_2\}(PF_6)_2$ was optimized as a reliability test for the computational optimization. Geometry optimizations and single point calculations were then done for $\{Cu[Cu(SL^2)(Cl)_2]_2\}^{2+}$, considering an unrestricted state with $S = 3/2$.

Electronic structure calculations have been performed under a DFT approximation. The single point calculations were obtained with the Gaussian 03 code[34a] using the hybrid B3LYP functional.[34b] We have employed a triple-ξ all-electron Gaussian basis set proposed by Schaefer et al. for all atoms.[35] A guess function was generated with the JAGUAR 5.5 code.[36] The methodology used for the calculations to obtain J (first neighbor interaction) was previously reported by Ruiz et al.[37−39]

Results and Discussion

Synthesis. The polypodal ligands HL^1, HSL^1, HL^2, and HSL^2 used in this work were synthesized through the Mannich reaction, which consists in the reaction of phenol or a substituted phenol and paraformaldehyde with a suitable amine (Scheme 2).

The elemental analysis and ^{1}H NMR correspond to the expected formula of the ligands.

Mononuclear Complexes 1−4. The synthesis of the mononuclear complexes was made straightforward by the reaction of copper(II) chloride solution with the ligand in a 1:1 molar ratio, in refluxing methanol for 1 h. The products crystallize after adding an excess of tetrabutylammonium hexafluorophosphate to the reaction mixture.

Description of the Crystal Structures. In all the described mononuclear complexes the ligand is protonated, contrary to the results observed for other similar systems, in which the ligand is deprotonated because of the presence of base in the reaction media, giving the corresponding phenolate complexes.[40] The mononuclear complexes **1**−**4** have all a monometallic cationic unit $[Cu(HL)Cl]^+$, counterbalanced with an hexafluorophosphate anion. For these compounds, the copper(II) center shows a coordination number of five, with four positions occupied by donor atoms from HL and one by a monodentate chlorine atom, as shown in Figure 1. Table 2 summarizes the selected distances and bond angles.

The coordination geometry of the metal center can be described as slightly distorted square pyramidal in all cases (τ[41] = 0.02, 0.22, 0.04, and 0.05 for **1**−**4**). The basal positions are occupied by three nitrogen atoms from the

(32) Verluis, L.; Ziegler, T. *J. Chem. Phys.* **1988**, *88*, 322–328.
(33) Manzur, J.; Mora, H.; Vega, A.; Spodine, E.; Venegas-Yazigi, D.; Garland, M.; El Fallah, M. S.; Escuer, A. *Inorg. Chem.* **2007**, *46*, 6924–6932.
(34) (a) Frisch et al. *Gaussian 03*, revision B4; Gaussian, Inc.: Pittsburgh, PA, 2003. (b) Becke, D. *J. Chem. Phys.* **1993**, *98*, 5648–5652.
(35) Schaefer, C.; Huber, R.; Ahlrichs, R. *J. Chem. Phys.* **1994**, *100*, 5829–5835.
(36) *Jaguar 5.5*; Schrödinger, Inc.: Portland, OR, 2003.
(37) Ruiz, E.; Cano, J.; Alvarez, S.; Alemany, P. *J. Comput. Chem.* **1999**, *20*, 1391–1400.
(38) Ruiz, E.; Rodriguez-Fortea, A.; Cano, J.; Alvarez, S.; Alemany, P. *J. Comput. Chem.* **2003**, *24*, 982–989.
(39) Ruiz, E. *Struct. Bonding* (*Berlin*) **2004**, *113*, 71–102.
(40) Itoh, S.; Taki, M.; Kumei, H.; Takayama, S.; Nagatomo, S.; Kitagawa, T.; Sakurada, N.; Arakawa, R.; Fukuzumi, S. *Inorg, Chem.* **2000**, *39*, 3708–3711.
(41) Addison, A. W.; Rao, T. N.; Reedijk, J.; Van Rijn, J.; Vershcoor, G. C. *J. Chem. Soc., Dalton Trans.* **1984**, 1349–1356.

Scheme 2. General Scheme for the Synthesis of the Ligands

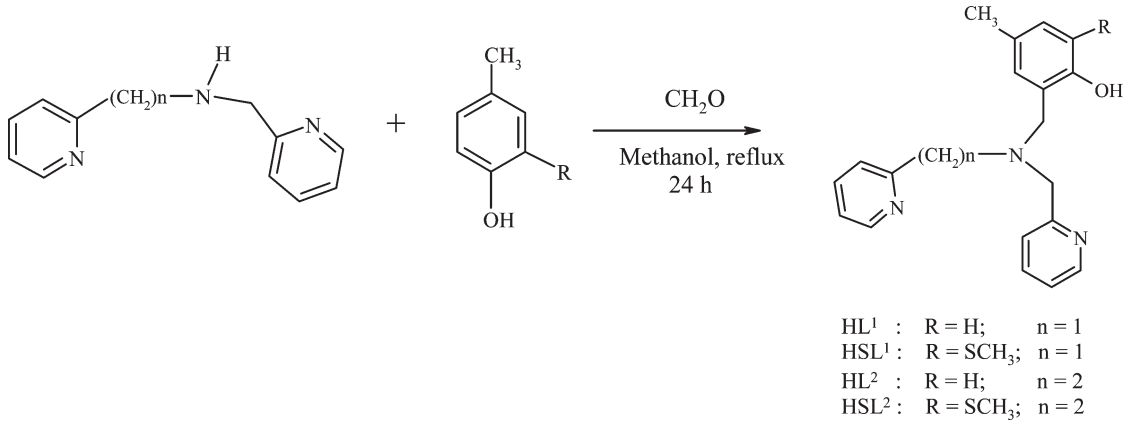

HL^1 : R = H; n = 1
HSL^1 : R = SCH_3; n = 1
HL^2 : R = H; n = 2
HSL^2 : R = SCH_3; n = 2

pyridine moiety and a chlorine atom. The apical position is occupied by the oxygen from the hydroxyl group of the phenol ligand. The axial coordination of the phenolate group has been observed for other systems with the 5,5,6 sequence of chelate rings. This is due to the greater steric effect which is imposed by the smaller rings.[16] For compounds with a ring sequence of 6,6,6, the phenolate ligand tends to occupy the equatorial position.[42−44]

Interestingly, the phenolate ring is not parallel to the Cu−O1 vector, defining an angle of 139.8(1)°, 43.9(1)°, 40.4(1)°, and 43.1(1)° for **1**, **2**, **3**, and **4**, respectively. The effect is that the mirror image of the molecule can not be superimposed with the molecule itself. Since the crystal system for these four molecules is centrosymmetric, the crystalline structure for each compound contains both isomers in a 1:1 ratio.

The pyridyl group nitrogen atoms are *trans* in all mononuclear compounds. Thus, the ligand acts as tetracoordinating moeity with a N_3O donor set. In all cases the copper atom deviates slightly from the basal coordination mean plane (N,N′,N″,Cl) in the direction of the apical oxygen atom (0.16, 0.03, 0.01, and 0.05 Å for **1**−**4**, respectively).

The introduction of an additional methylene group between the pyridyl group and the aliphatic nitrogen atom N2 in **3** and **4** in comparison with **1** and **2**, modifies the chelating ring system from a 5,5,6 to a 5,6,6, and is reflected in the decrease of the N2−Cu−N3 angle going from 90.95(9)° and 91.87(13)° (**3** and **4**) to 82.25(14)° and 83.5(2)° (**1** and **2**).

The incorporation of a SCH_3 group within the phenolic ring in **2** and **4** does not cause major perturbations in the ligand coordination geometry, being similar to that observed for **1** and **2**. The sulfur atom of the thiomethyl substituent (S1) is at a distance of 5.030(1) Å and 4.951(1) Å from the central copper atom in **2** and **4**, respectively. These values are indicative of the absence of a Cu−S coordination bond. The methyl group is out of the plane of the phenolic ring, so that the C14−C15−S1−C18 and C16−C15−S1−C18 torsion angles are 61.1(8)° and −118.3(7)° for **2** and 45.1(5)° and −134.2(4)° for **4**. These values for the out-of-the-plane torsion angle are unusual, since in compounds without a Cu−S bond this group is expected to be approximately coplanar with the aromatic ring.[44] The torsion observed may be attributed to packing effects; a compact packing demands the methyl-sulfur group to be out of the plane.

For all the studied monomeric species the apical phenyl ring is out of the direction of the Cu−O vector; this fact is reflected in the measured values for the Cu−O1−C16 angle: 112.3(2)°, 112.2(2)°, 110.9(2)°, and 114.5(2)° for **1**−**4**, respectively.

The crystal packing does not show significant interactions between the $[Cu(HL^x)Cl]^+$ units, but the presence of a hydrogen atom in the phenolic O−H group leads to a hydrogen bond with a methanol oxygen atom from solvent in **1** (O1···O100 ($x - 1$, y, z) 2.619(5) Å) and **3** (O1···O100 2.648(3) Å). The packing of the compounds also shows a set of F···H−C contacts.

Electrochemical Behavior. The redox behavior of the complexes **1**−**4** was studied by cyclic voltammetry, using acetonitrile as the solvent. The CV curve of the free ligands displays irreversible anodic signals, as expected for phenol-centered electron transfer. Oxidation of the phenol to its phenoxyl radical occurs at a high potential ranging from 550 to 800 mV (vs SCE) usually found for this type of ligand.[45,46] The observed cyclic voltammograms for the mononuclear species show a reduction signal in the range of −70 to −200 mV, corresponding to the Cu^{II}/Cu^{I} couple, in addition to an irreversible oxidation signal at approximately 1500 mV (ill defined) for **1** and **3**, and about 1300 mV, for **2** and **4**, corresponding to the oxidation of the phenolic moiety leading to unstable radical cations, undoubtedly of the phenoxyl type. Oxidation occurs at higher potentials relative to the free ligands because of the positive charge on the copper atom, which decreases the electron density on the phenolic unit and thus makes it less easily oxidizable. Table 3 summarizes the obtained results and Supporting Information, Figure 1S shows a typical voltammogram for complex $[Cu(HSL^1)Cl]PF_6 \cdot 0.75H_2O$ (**2**).

(42) Karlin, K. D.; Cohen, B. I.; Hayes, J. C.; Farooq, A.; Zubieta, J. *Inorg. Chem.* **1987**, *26*, 147–153.
(43) Adams, H.; Bailey, N. A.; Fenton, D. E.; He, Q.-Y.; Ohba, M.; Okawa, H. *Inorg. Chim. Acta* **1994**, *215*, 1–3.
(44) Adams, H.; Bailey, N. A.; Rodriguez de Barbarin, C. O.; Fenton, D. E.; He, Q.-Y. *J. Chem. Soc., Dalton Trans.* **1995**, 2323–2331.
(45) Romanowski, S.; Tormena, F.; Dos Santos, V.; Hermann, M.; Mangrich, A. *J. Braz. Chem. Soc.* **2004**, *15*, 897–903.
(46) Philibert, A.; Thomas, F.; Philouze, C.; Hamman, S.; Saint-Aman, E.; Pierre, J.-L. *Chem.—Eur. J.* **2003**, *9*, 3803–3812.

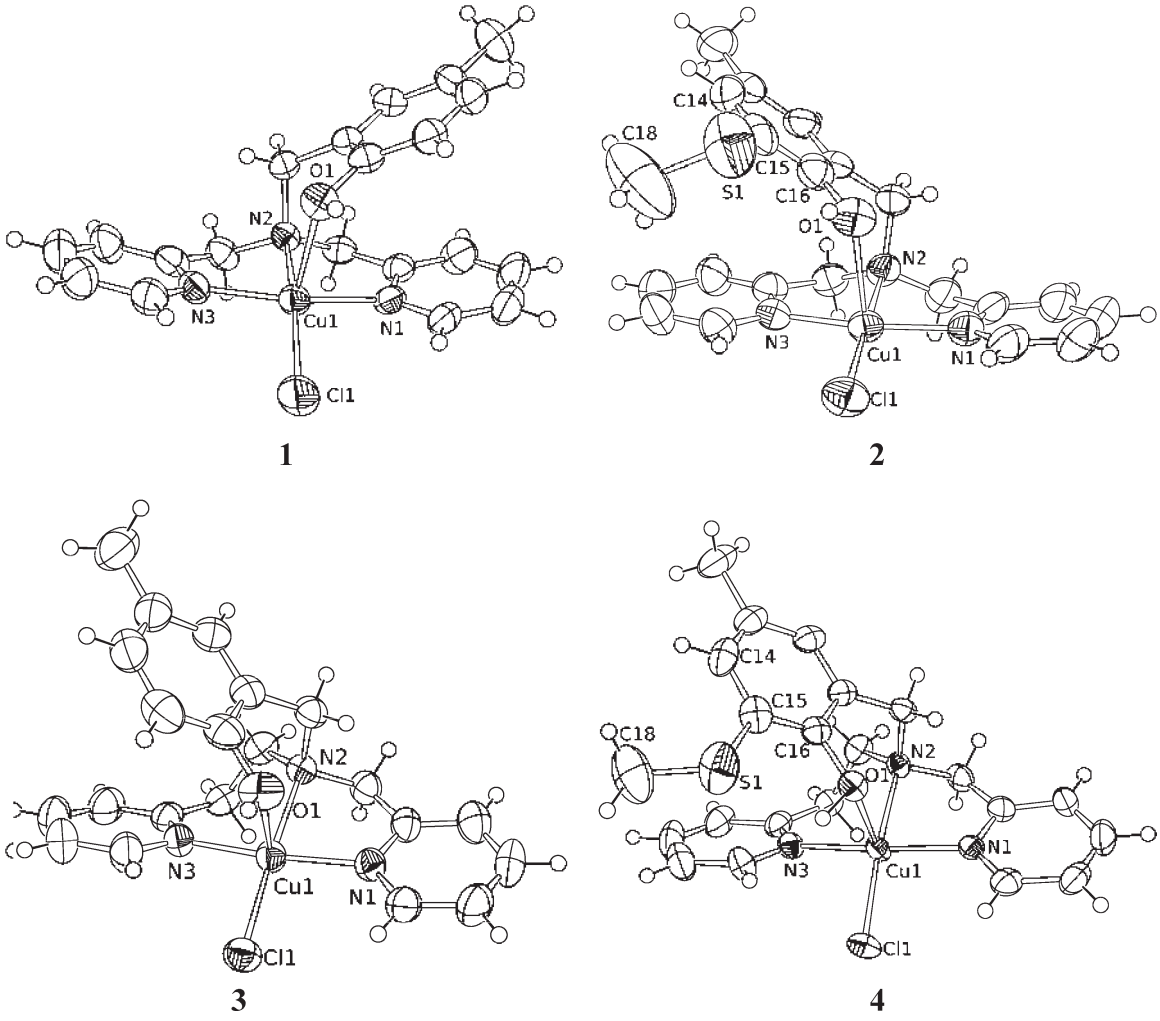

Figure 1. Molecular diagrams of mononuclear species. **1**: $[Cu(HL^1)Cl](PF_6)$; **2**: $[Cu(HSL^1)Cl](PF_6)$; **3**: $[Cu(HL^2)Cl](PF_6)$; **4**: $[Cu(HSL^2)Cl]PF_6$. Solvent molecules and counteranions have been omitted for clarity. Displacement ellipsoids at the 50% level of probability and hydrogen atoms are shown as spheres of arbitrary radii.

The reduction potential of the mononuclear species shows a shift toward more positive values for the complexes with the thiomethyl substituted ligands, for example, −213 mV and −184 mV for Cu-HL^1 and Cu-HSL^1, respectively. When comparing the Cu−O(phenol) distances in these two complexes it is possible to observe that the distance for the complex with the sulfur substituent is greater. The longer Cu−O distance may be due to the steric effect resulting from the hindrance of the thiomethyl group toward one of the pyridyl groups. This would mean a smaller electron density on the copper center that leads to a more positive reduction potential as compared with the complex with the non-sulfured ligand. The effect of the thiomethyl substituents on the redox potential of the phenolic group is reflected in a decrease of about 200 mV. The thioether bond may facilitate delocalization of the spin density of the free radical, thus lowering the redox potential. It has been reported that thioether substitution may lead to a decrease in redox potential of 0.5 V or more.[47−49]

The effect of the increase in the length of the alkyl chain is reflected in an increase of the reduction potential of the copper center, −213 mV and −142 mV for Cu-HL^1 and Cu-HL^2, respectively. Literature reports that ligands which form a five-member chelate ring stabilize better the copper(II) oxidation state, in comparison with those that form a six-member chelate ring.[7] However, the oxidation potential of the phenol group is not significantly altered.

UV−visible Spectroscopy. After dissolution of the mononuclear protonated complexes in acetonitrile, only d-d transitions were observed in the visible region of the electronic spectrum. All the studied complexes present a low intensity absorption band at approximately 600 nm (Supporting Information, Figure 2S). Table 3 summarizes the maximum wavelengths of the absorption bands.

Since the phenolic group is protonated, the charge transfer band corresponding to phenolate to copper ligand-to-metal charge transfer (LMCT) is not observed in the 400 nm region for the studied complexes. The variation of the absorption band maxima can be related

(47) Whittaker, M. M.; Chuang, Y. Y.; Whittaker, J. W. *J. Am. Chem. Soc*. **1993**, *115*, 10029–10035.
(48) Whittaker, M. M.; Duncan, W. R.; Whittaker, J. W. *Inorg. Chem*. **1996**, *35*, 382–386.
(49) Itoh, S.; Hirano, K.; Furuta, A.; Komatsu, M.; Ohshiro, Y.; Ishida, A.; Takamuku, N.; Suzuki, S. *Chem. Lett*. **1993**, 2099–2102.

Table 2. Selected Bond Distances (Å) and Angles (deg) for Complexes **1**, **2**, **3**, and **4**

$[Cu(HL^1)Cl]PF_6 \cdot CH_3OH$ (**1**)		$[Cu(HSL^1)Cl]PF_6 \cdot 0.75\ H_2O$ (**2**)	
Cu1−O1	2.365(3)	Cu1−O1	2.466(5)
Cu1−N1	1.976(3)	Cu1−N1	1.988)(5)
Cu1−N2	2.032(3)	Cu1−N2	2.026(5)
Cu1−N3	1.976(3)	Cu1−N3	1.967(2)
Cu1−Cl1	2.2332(12)	Cu1−Cl1	2.241(2)
		Cu1 S1	5.030(1)
N1−Cu1−O1	87.95(12)	N1−Cu1−N2	82.8(2)
N1−Cu1−N2	83.26(13)	N1−Cu1−N3	166.1(2)
N1−Cu1−N3	165.22(14)	N1−Cu1−O1	94.8(2)
N1−Cu1−Cl1	97.21(10)	N1−Cu1−Cl1	96.58(16)
N2−Cu1−O1	88.29(11)	N2−Cu1−N3	83.5(2)
N2−Cu1−N3	82.25(14)	N2−Cu1−O1	87.1(2)
N2−Cu1−Cl1	166.66(10)	N2−Cu1−Cl1	178.99(15)
N3−Cu1−O1	94.45(13)	N3−Cu1−O1	87.3(2)
N3−Cu1−Cl1	96.23(11)	N3−Cu1−Cl1	97.01(16)
O1−Cu1−Cl1	105.04(8)	O1−Cu1−Cl1	93.7(2)
$[Cu(HL^2)Cl]PF_6 \cdot CH_3OH$ (**3**)		$[Cu(HSL^2)Cl]PF_6 \cdot 1.5\ CH_3OH$ (**4**)	
Cu1−O1	2.405(2)	Cu1−O1	2.405(2)
Cu1−N1	2.006(2)	Cu1−N1	2.006(2)
Cu1−N2	2.098(2)	Cu1−N2	2.098(2)
Cu1−N3	1.990(2)	Cu1−N3	1.990(2)
Cu1−Cl1	2.3038(8)	Cu1−Cl1	2.3038(8)
		Cu1 S1	4.951(1)
N1−Cu1−O1	87.80(9)	N1−Cu1−N2	81.98(13)
N1−Cu1−N2	81.62(9)	N1−Cu1−N3	172.35(14)
N1−Cu1−N3	171.88(9)	N1−Cu1−O1	92.84(12)
N1−Cu1−Cl1	94.45(7)	N1−Cu1−Cl1	93.19(11)
N2−Cu1−O1	87.27(8)	N2−Cu1−N3	91.87(13)
N2−Cu1−N3	90.95(9)	N2−Cu1−O1	87.09(11)
N2−Cu1−Cl1	174.52(6)	N2−Cu1−Cl1	175.14(9)
N3−Cu1−O1	95.13(9)	N3−Cu1−O1	91.38(12)
N3−Cu1−Cl1	93.18(7)	N3−Cu1−Cl1	92.90(11)
O1−Cu1−Cl1	88.78(6)	O1−Cu1−Cl1	93.75(8)

Table 3. Electronic Properties and Redox Potentials for the Studied Complexes[a]

	electronic absorption	E_{redox} (metal)[b]		E_{redox} (ligand)
complex	λ_{Max} (ε, $M^{-1}\ cm^{-1}$)	E_c (mV)	E_a (mV)	E_a (mV)
$[Cu(HL^1)Cl]PF_6\ CH_3OH$ (**1**)	630(333)	−213	−94	1500
$[Cu(HSL^1)Cl]PF_6 \cdot 0.75\ H_2O$ (**2**)	680(93)	−184	−72	1320
$[Cu(HL^2)Cl]PF_6\ CH_3OH$ (**3**)	600(224)	−142	20	1550
$[Cu(HSL^2)Cl]PF_6\ 2CH_3OH$ (**4**)	620(123)	−73	61	1360

[a] Working electrode: glassy carbon; reference: saturated calomel electrode; supporting electrolyte: 0.1 M tetrabutylammonium hexafluorophosphate in acetonitrile. Scan rate: 100 mV s^{-1}. [b] E_c, E_a: midpoints of cathodic and anodic waves.

with the ligand structure, mainly with the thiomethyl group and the alkyl chain length. The effect of the thiomethyl group is reflected on a shift of the band toward lower energy values, as it has been reported for similar copper complexes.[50] In contrast, an increase in the alkyl chain length and therefore an increase in the ligand flexibility causes a shift toward greater energies.

Polynuclear Complexes. $[Cu_2(SL^2)_2](PF_6)_2 \cdot 2CH_3OH$ (**5**) and $\{[CuSL^2(Cl)]_2Cu\}(PF_6)_2$ (**6**).

Description of the Crystal Structures. $[Cu_2(SL^2)_2](PF_6)_2 \cdot 2CH_3OH$ (5). Compound **5** corresponds to a dinuclear copper unit, $[Cu_2(SL^2)_2]^{2+}$, counterbalanced by two hexafluorophosphate anions. Although the formula as presented suggests internal symmetry, the two cupric centers in the cation are slightly different. Three nitrogen atoms from the ligand are part of the first coordination sphere of the copper centers, each in a square base pyramidal environment (τ = 0.13 for Cu1 and 0.00 for Cu10). For Cu1 the basal plane is defined by N1, N2, O1, and O10, while for Cu10 it is defined by N10, N20, N30, and O1. Besides, a long distance interaction is observed for Cu10 with S1 (2.867(2) Å). Both centers are connected

(50) Halfen, J. A.; Jazdzewski, B. A.; Mahapatra, S.; Berreau, L. M.; Wilkinson, E. C.; Que, L., Jr.; Tolman, W. B. *J. Am. Chem. Soc.* **1997**, *119*, 8217–8227.

Table 4. Selected Bond Distances (Å) and Angles (deg) for Complex **5**

$[Cu_2(SL^2)_2](PF_6)_2 \cdot 2CH_3OH$ (**5**)

Cu1−O10	1.911(3)	Cu10−O10	2.246(3)
Cu1−O1	2.039(3)	Cu10−O1	2.031(3)
Cu1−N1	2.056(4)	Cu10−N10	2.019(3)
Cu1−N2	1.998(4)	Cu10−N20	2.072(4)
Cu1−N3	2.332(3)	Cu10−N30	2.032(3)
Cu1−S10	2.867(4)	Cu10−S1	3.180(1)
N1−Cu1−O1	175.66(13)	N10−Cu10−N20	82.20(15)
N1−Cu1−N2	85.06(15)	N10−Cu10−N30	161.98(13)
N1−Cu1−N3	81.28(13)	N10−Cu10−O1	94.28(13)
N1−Cu1−O10	100.28(14)	N10−Cu10−O10	100.53(12)
N2−Cu1−O1	93.35(13)	N20−Cu10−N30	94.65(14)
N2−Cu1−N3	92.00(14)	N20−Cu10−O1	161.88(12)
N2−Cu1−O10	166.93(14)	N20−Cu10−O10	90.01(12)
N3−Cu1−O1	102.83(12)	N30−Cu10−O1	93.94(13)
N3−Cu1−O10	100.57(12)	N30−Cu10−O10	97.20(12)
O1−Cu1−O10	80.44(11)	O1−Cu10−O10	73.09(10)

in a μ-fashion by two phenoxo oxygen atoms. The two phenoxo bridges are different: O1 bridges the copper centers in an equatorial-equatorial fashion, while O10 is an equatorial(Cu1)-axial(Cu10) bridge. Each copper is slightly deviated from its respective least-squares basal plane (0.14 for Cu1 and 0.00 Å for Cu10) which defines a dihedral angle of 94.3(2)°. Table 4 shows selected bond distances and angles for **5**, while Figure 2 shows a molecular diagram of the bimetallic cationic unit $[Cu_2(SL^2)_2]^{2+}$.

$\{[CuSL^2(Cl)]_2Cu\}(PF_6)_2$ (6). As described in the literature $\{[CuSL^1(Cl)]_2Cu\}^{2+}$[33] is a trinuclear copper complex bearing two $[CuSL^1(Cl)]$ units coordinating a central copper(II) center through O, S, and Cl atoms. Since efforts to crystallyze the $\{[CuSL^2(Cl)]_2Cu\}^{2+}$ analogue, being reported in this work, were unsuccessful (see Experimental Section), a DFT optimization was carried out to get an insight into the structure. Table 5 shows selected bonds and angles measured for $\{[CuSL^1(Cl)]_2Cu\}(PF_6)_2$,[33] and the corresponding DFT calculated values for comparison, together with the geometric results for $\{[CuSL^2(Cl)]_2Cu\}^{2+}$ (**6**). Figure 3 shows a molecular structure diagram for $\{[CuSL^2(Cl)]_2Cu\}^{2+}$ as optimized from DFT calculations.

As it becomes evident from data in Table 5 and Figure 3, important structural changes occur in the $\{[CuSL^n(Cl)]_2Cu\}^{2+}$ cations when HSL^1 is replaced by HSL^2. The scheme of the molecule is maintained, with a central copper(II) ion coordinated by $[CuSL^n(Cl)]$ units. One difference occurs in the coordination sphere of the terminal cupric centers inside this unit. This can be well described as an square-base pyramid ($\tau = 0.26$) for $\{[CuSL^1(Cl)]_2Cu\}^{2+}$, while for $\{[CuSL^2(Cl)]_2Cu\}^{2+}$ the geometry is distorted, being between SBP and TBP as reflected by the computed τ-value of 0.48. The presence of a methylene group in one of the ligand arms of **6** leads to a change in the bite angle (N2−Cu1−N3), from about 83° for the reported complex to 95° for **6**. Also important changes occur in the geometry of the central Cu2 atom; a distorted tetrahedral CuO_2S_2 core for HSL^1, while a more distorted tetrahedral CuO_2Cl_2 core for HSL^2 can be observed. It is important to point out the existence of two bridges (one chloride and one phenoxo) between the central and each of the peripherical cupric ions in $[CuSL^2(Cl)]$ in **6**, permitting the prediction that the magnetic behavior will be somewhat different to that reported for the $\{[CuSL^1(Cl)]_2Cu\}^{2+}$ analogue.[33]

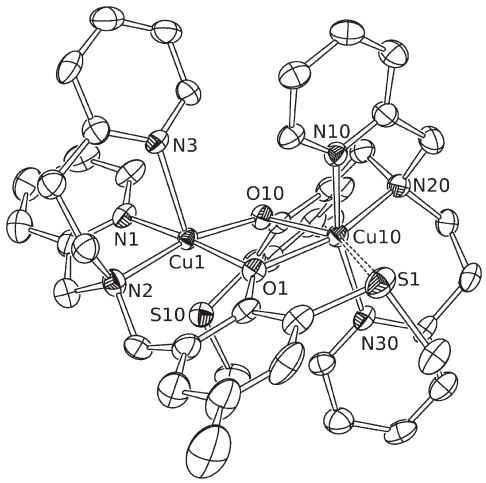

Figure 2. Molecular diagram of the $[Cu_2(SL^2)_2]^{2+}$ cation for (**5**). Counteranions and hydrogen atoms have been omitted for clarity. Displacement ellipsoids at the 50% level of probability.

Magnetic Properties. $[Cu_2(SL^2)_2](PF_6)_2$ (5). Molar magnetic susceptibility at variable temperatures was determined at 0.1 T. Figure 4a shows the χ_M versus T and $\chi_M T$ versus T dependence obtained for **5**, indicating the existence of antiferromagnetic interactions between the copper(II) centers.

The value of $\chi_M T$ at 291 K is of 0.69 $cm^3\ mol^{-1}$ K, which is lower than the expected value for two uncoupled copper(II) ions (0.75 $cm^3\ mol^{-1}$ K, with $g = 2$). The value of $\chi_M T$ decreases continuously from 291 K (0.69 $cm^3\ mol^{-1}$ K) to 40 K (0.03 $cm^3\ mol^{-1}$ K); below this temperature the $\chi_M T$ values remain constant, with values close to zero. The χ_M value at 291 K is of 0.0024 $cm^3\ mol^{-1}$ which increases continuously to reach a maximum value of 0.0034 $cm^3\ mol^{-1}$ at 130 K; at low temperature a small paramagnetic contribution ($\propto 1/T$) is observed.

The experimental data were fitted with the Bleaney−Bowers expression, using the isotropic exchange Hamiltonian, $H = -J\hat{S}_1 \cdot \hat{S}_2$, for two interacting copper centers with $\hat{S}_1 = \hat{S}_2 = 1/2$, and a small paramagnetic impurity contribution. The calculated χ_M can be obtained by eq 1,[51] where the symbols have their usual meaning.

$$\chi_M = \frac{2N\beta^2 g^2}{kT[3 + \exp(-J/kT)]}(1-\rho) + \frac{N\beta^2 g^2}{2kT}\rho \qquad (1)$$

The calculated curve matches well with the experimental data in the all temperature range. The best fit parameters from 286 down to 2.3 K are found to be $J = -134\ cm^{-1}$ and $g = 2.07$, and $\rho = 0.05\%$ with an agreement factor $R = \sum[(\chi_M T)_{exp} - (\chi_M T)_{calc}]^2/\sum[(\chi_M T)_{exp}]^2$ of 5.6×10^{-5}.

This result is similar to other copper(II) antiferromagnetic dinuclear complexes such as bis(μ-phenoxo)-dicopper(II) complexes.[52] Moreover, Chaudhuri et al.[53] divided the magnetic behavior in four groups according

(51) Kahn, O. In *Molecular Magnetism*; Wiley-VCH Inc.: New York, 1993.

Table 5. Selected Bond Distances (Å) and Angles (deg) for $\{[CuSL^1(Cl)]_2Cu\}(PF_6)_2$,[33] (Measured and DFT-Optimized) and the Corresponding Optimized Values for $\{[CuSL^2(Cl)]_2Cu\}^{2+}$ (**6**)

X-ray data for $\{[CuSL^1(Cl)]_2Cu\}(PF_6)_2$		[a]DFT data for $\{[CuSL^1(Cl)]_2Cu\}^{2+}$	[a]DFT data for $\{[CuSL^2(Cl)]_2Cu\}^{2+}$(**6**)
Cu1−O1	2.256(4)	2.312	2.312
Cu2−O1	1.913(4)	2.018	2.277
Cu1−N1	1.989(5)	2.049	2.093
Cu1−N2	1.983(5)	2.151	2.236
Cu1−N3	2.052(4)	2.050	2.116
Cu1−Cl1	2.252(2)	2.290	2.459
Cu2−Cl1	3.173(2)	3.144	2.321
Cu2−S1	2.294(2)	2.402	3.117
Cu1−Cu2	3.4867(9)	3.577	3.465
Cu1−Cu1′	5.7722(15)	5.984	6.109
N1−Cu1−N2	159.0(2)	154.0	135.3
N1−Cu1−N3	81.8(2)	81.4	80.8
N2−Cu1−N3	83.3(2)	82.3	95.2
N2−Cu1−Cl1	96.8(2)	97.9	96.1
N3−Cu1−Cl1	174.4(1)	178.4	164.7
O1−Cu1−Cl1	93.1(1)	91.9	78.2
O1−Cu2−S1	88.6(1)	85.4	
O1−Cu2−Cl1			81.8
O1−Cu2−Cl1′			95.7
S1−Cu2−S1′	97.0(1)	101.0	80.7
Cu1−O1−Cu2	113.3(2)	111.3	98.0
Cu1−Cl1−Cu2			92.9
Cu1−Cu2−Cu1′	111.74(4)	113.5	123.7

[a] Since the optimized structure has no C_i symmetry, the terminal copper atoms have slightly different geometries. The reported values correspond to the average, but the maximun deviations do not exceed 0.005 Å or 0.9°.

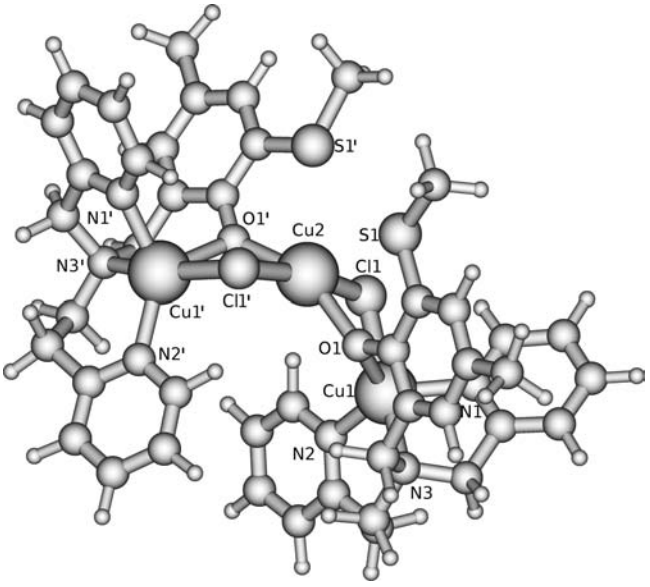

Figure 3. DFT-optimized geometry for $\{[CuSL^2(Cl)]_2Cu\}^{2+}$.

with the nature and strength of the exchange coupling observed in these bis(μ-phenoxo)dicopper(II) complexes: (i) $-J > 0$; (ii) $-J \leq 50$; (iii) $-J \leq 50-150$, and (iv) $-J \geq 150$ cm^{-1}. Many complexes present moderate to strong antiferromagnetic interactions (groups iii and iv), with Cu−O(Ph)−Cu angles greater of 97°. In the case of compound **5** the phenoxo groups are bridging the copper centers in an axial−equatorial and equatorial−equatorial mode. The dominant antiferromagnetic exchange interaction found in this compound should be related to the equatorial−equatorial configuration of one of the phenoxo bridges, (the average angle being 102.58°) because of the better overlap between the $d_{x^2-y^2}$ orbitals of the copper ions and the corresponding orbitals of the bridge in the equatorial-equatorial mode.[54−57]

On the other hand, the obtained results are completely different to those reported in a previous work for similar binuclear complexes. For the reported[33] $[Cu_2(SL^1)_2](PF_6)_2$, where HSL^1= 2-[(bis(2-pyridylmethyl)amino)-methyl]-4-methyl-6-(methylthio)phenol, the authors found that a weak ferromagnetic interaction appears as the dominant behavior, with a J value of +3.4 cm^{-1}. The small positive value of J was attributed mainly to the fact that copper(II) centers are bridged by two phenoxo groups in an axial−equatorial fashion, which does not allow strong interactions between the metal centers.[58]

$\{[CuSL^2(Cl)]_2Cu\}(PF_6)_2$ (6). Molar magnetic susceptibility data at variable temperature of **6** were determined at 0.1 T in the temperature range of 2.5 to 275 K.

(52) Selected recent examples: (a) Chiari, B.; Piovesana, O.; Tarantelli, T.; Zanazzi, P. F. *Inorg. Chem.* **1988**, *27*, 4149–4153. (b) Mandal, S. K.; Thompson, L. K.; Newlands, M. J.; Gabe, E. J.; Nag, K. *Inorg. Chem.* **1990**, *29*, 1324–1327. (c) Berti, E.; Caneschi, A.; Daiguebonne, C.; Dapporto, P.; Formica, M.; Fusi, V.; Giorni, L.; Guerri, A.; Micheloni, M.; Paoli, P.; Pontellini, R.; Rossi, P. *Inorg. Chem.* **2003**, *42*, 348–357. (d) Paschke, R.; Liebsch, S.; Tschierske, C.; Dakley, A.; Sinn, E. *Inorg. Chem.* **2003**, *42*, 8230–8240. (e) Saimiya, H.; Sunatsuki, Y.; Kojima, M.; Kashino, S.; Kambe, T.; Hirotsu, M.; Akashi, H.; Nakajima, K.; Tokii, T. *J. Chem. Soc., Dalton Trans.* **2002**, 3737–3742 and references therein.
(53) Chaudhuri, P.; Wagner, R.; Weyhermüller, T. T. *Inorg. Chem.* **2007**, *46*, 5134–5136.
(54) Thompson, L. K.; Mandal, S. K.; Tandon, S. S.; Bridson, J. N.; Park, M. K. *Inorg. Chem.* **1996**, *35*, 3117–3125.
(55) Felthouse, T. R.; Laskowski, E. J.; Hendrickson, D. N. *Inorg. Chem.* **1977**, *16*, 1077–1089.
(56) Hay, P. J.; Thibeault, J. C.; Hoffmann, R. *J. Am. Chem. Soc.* **1975**, *97*, 4884–4899.
(57) Doman, T. N.; Williams, D. E.; Banks, J. F.; Buchanan, R. M.; Chang, H.-R.; Webb, R. J.; Hendrickson, D. N. *Inorg. Chem.* **1990**, *29*, 1058–1062.
(58) Berends, H. P.; Stephan, D. W. *Inorg. Chem.* **1987**, *26*, 749–754.

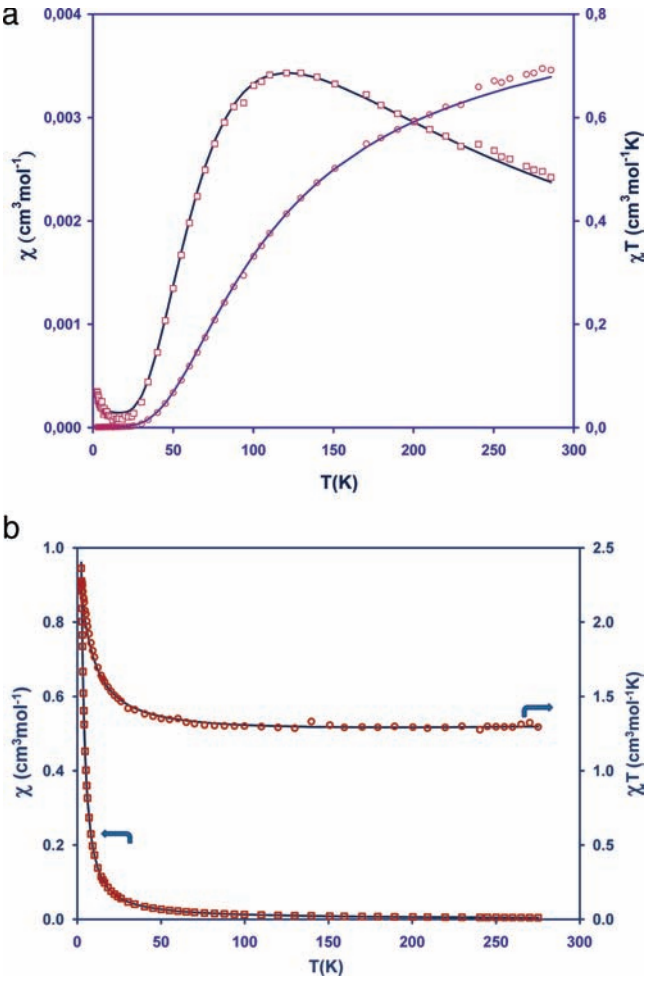

Figure 4. (a) χ_M and $\chi_M T$ vs T dependence for $[Cu_2(SL^2)_2](PF6)_2$ (**5**). (b) χ_M and $\chi_M T$ vs T dependence for $\{[CuSL^2(Cl)]_2Cu\}(PF_6)_2$ (**6**).

Figure 4b shows the χ_M versus T and $\chi_M T$ versus T dependence obtained for **6**. The existence of a ferromagnetic interaction between the copper(II) centers can be inferred from the increase of the $\chi_M T$ values at low temperatures. The value of $\chi_M T$ at 275 K is 1.30 cm^3 mol^{-1} K, which is slightly higher than the expected value for three uncoupled copper(II) centers (1.125 cm^3 mol^{-1} K, with $g = 2$). The $\chi_M T$ value remains practically constant between 275−80 K; below this temperature the value increases continuously, reaching 2.26 cm^3 mol^{-1} K at 2.5 K.

Since this complex corresponds to a trinuclear unit, and following the reference given by Manzur et al.,[33] we tried to fit the observed magnetic data using the expression derived from the Hamiltonian $H = -J(\hat{S}_1 \cdot \hat{S}_2 + \hat{S}_2 \cdot \hat{S}_3) - J'(\hat{S}_1 \cdot \hat{S}_3)$ given by the following equation:

$$\chi_M = \frac{N\beta^2}{4kT}\left[\frac{g^2{}_{1/2,1} + g^2{}_{1/2,0}\exp[(J-J')/kT)] + 10g^2{}_{3/2,1}\exp[3J/2kT]}{1+\exp[(J-J')/kT + 2\exp[3J/2kT]]}\right] \quad (2)$$

with $g_{1/2,1} = (4g_1 - g_2)/3$; $g_{3/2,1} = (2g_1 + g_2)/3$; $g_{1/2,0} = g_2$ and where J corresponds to the magnetic interaction between the first neighbor copper(II) centers, and J' to the exchange interaction between the second neighbor copper(II) centers.

For the studied complex we were able to fit the data using a simplified model, considering $J' = 0$ and $g_1 = g_2$. The best fit parameters were $g = 2.08$ and $J = +11.9\ cm^{-1}$. This J value is of the order of the observed one for the analogous trinuclear complex using HSL^1 as ligand ($J = +5.7\ cm^{-1}$).[33] Even though the phenoxo bridging angle Cu−O−Cu is 113.3° for the cited complex, and 98.0° for the optimized structure of **6**, this difference in angles should not be used as an explanation to justify the small difference in the above-mentioned J values.

The geometry optimization of compound **6** gave a structure showing two different exchange pathways between each terminal copper atom and the central atom, that is, a phenoxo and a chloro bridge. Even though the guess structure used in the optimization of compound **6** presents only one phenoxo bridge between the central and each terminal copper atom, in the final calculated structure, the chloro atoms become part of the coordination sphere of the central atom and also act as bridges. On the basis of the fact that the calculated structure of **6** has two terminal copper(II) centers with slightly different geometries, two first neighbor magnetic interactions were obtained using DFT calculations giving a value of $J_1 = +72.8$ and $J_2 = +61.4\ cm^{-1}$. These values confirm that the obtained coordination spheres and the bridging atoms produce a ferromagnetic behavior for **6**. Therefore, we propose that the first coordination sphere of **6** corresponds to the calculated one. Nevertheless, it is important to note that the bond distances and angles in the solid state may differ slightly from the ones reported in this work.

Conclusions

Four mononuclear complexes $[Cu(HL^1)Cl]PF_6 \cdot CH_3OH$ (**1**), $[Cu(HSL^1)Cl]PF_6 \cdot 0.75H_2O$ (**2**), $[Cu(HL^2)Cl]PF_6 \cdot CH_3OH$ (**3**), $[Cu(HSL^2)Cl]PF_6 \cdot 1.5\ CH_3OH$ (**4**), and two polynuclear complexes $[Cu_2(SL^2)_2](PF_6)_2 \cdot 2CH_3OH$ (**5**) and $Cu[Cu(SL^2)(Cl)]_2](PF_6)_2$ (**6**) were obtained and characterized.

In complexes **2** and **4** the thiomethyl group is not coordinated to the metal. However, in complex **5** the thiomethyl groups are at distances of 2.867(4) and 3.180(1) Å, the first indicating a weak bonding interaction. In complex **6** the proposed structure, obtained from DFT calculations, shows that the thiomethyl groups are not part of the coordination sphere of the copper centers.

Redox potential values for the Cu(II)/Cu(I) couple show the effect of the chelating ring size (−213 mV and −142 mV for Cu-HL^1 and Cu-HL^2, respectively) and the presence of the thiomethyl substituent (−213 mV and −184 mV for Cu-HL^1 and Cu-HSL^1, respectively). However, the irreversible oxidation potential of the phenol group is not significantely altered.

Acknowledgment. Financial support from projects FONDECYT 1050484 and ENL 08/03 (Vicerrectoría de Investigación and Desarrollo, Universidad de Chile) is gratefully acknowledged.

Supporting Information Available: Figure 1S, cyclic voltammogram for complex $[Cu(HSL^1)Cl]PF_6 \cdot 0.75\ H_2O$, and Figure 2S, UV−visible spectrum for the complex $[Cu(HL^1)Cl]PF_6 \cdot CH_3OH$ in acetonitrile. Crystallographic data for complexes **1** to **5** in CIF format. This material is available free of charge via the Internet at http://pubs.acs.org.